

1269393

THE UNITED STATES OF AMERICA

TO ALL TO WHOM THESE PRESENTS SHALL COME

UNITED STATES DEPARTMENT OF COMMERCE

United States Patent and Trademark Office

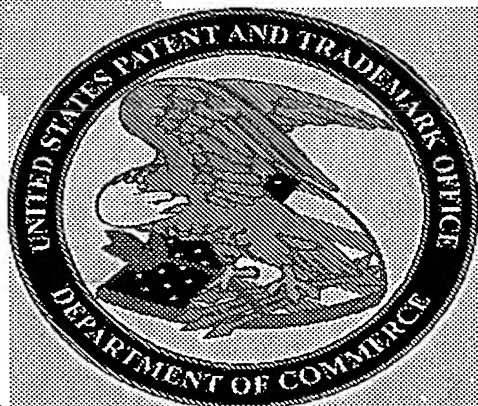
January 05, 2005

THIS IS TO CERTIFY THAT ANNEXED HERETO IS A TRUE COPY FROM THE RECORDS OF THE UNITED STATES PATENT AND TRADEMARK OFFICE OF THOSE PAPERS OF THE BELOW IDENTIFIED PATENT APPLICATION THAT MET THE REQUIREMENTS TO BE GRANTED A FILING DATE.

APPLICATION NUMBER: 60/510,707

FILING DATE: *October 10, 2003*

RELATED PCT APPLICATION NUMBER: PCT/US04/33602



Certified By

Jon W Dudas

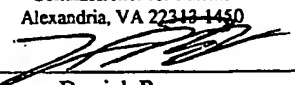
Under Secretary
of Commerce for Intellectual Property
and Acting Director of the
United States Patent and Trademark Office

PROVISIONAL APPLICATION COVER SHEET

This is a request for filing a PROVISIONAL APPLICATION under 37 CFR §1.53 (b)(2).

Attorney Docket No.: 5119-13000/D-2690-STE

INVENTOR(s)/APPLICANT(s)			
LAST NAME	FIRST NAME	MIDDLE INITIAL	RESIDENCE (City and either State or Foreign Country)
Maldonado	Stephen		Austin, TX USA
Stevenson	Keith	T.	Austin, TX USA

TITLE OF THE INVENTION (280 characters max) CARBON NANOTUBE-BASED ELECTROCATALYTIC ELECTRODES		CERTIFICATE OF EXPRESS MAIL UNDER 37 C.F.R. § 1.10 "Express Mail" label number: <u>EV324270544US</u> DATE OF DEPOSIT: <u>October 10, 2003</u> I hereby certify that this paper or fee is being deposited with the United States Postal Service "Express Mail Post Office to Addressee" Service Under 37 C.F.R. § 1.10 on the date indicated above and is addressed to: MAIL STOP PROVISIONAL APPLICATION Commissioner for Patents Alexandria, VA 22313-1450  Derrick Brown	
CORRESPONDENCE ADDRESS PH. (512) 853-8800 Eric B. Meyertons Meyertons, Hood, Kivlin, Kowert & Goetzel, P.C. P.O. Box 398 Austin, TX 78767-0398			
CITY, STATE Austin, Texas	ZIP CODE 78767-0398	COUNTRY U.S.A.	

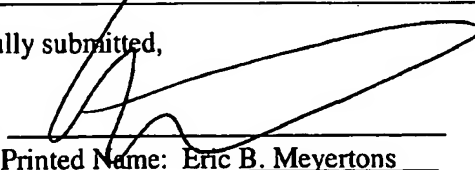
ENCLOSED APPLICATION PARTS (check all that apply)			
<input checked="" type="checkbox"/> Specification	18 pages	<input checked="" type="checkbox"/> Claims	2 pages
		(claims 1-11)	
<input checked="" type="checkbox"/> Title page	1 page	<input checked="" type="checkbox"/> Abstract	1 page
<input checked="" type="checkbox"/> Drawings	9 pages		
		(figures 1-9)	

METHOD OF PAYMENT (check one)	
<input checked="" type="checkbox"/> A fee authorization is enclosed to cover the Provisional filing fees	
<input type="checkbox"/> The Commissioner is hereby authorized to charge filing fees and credit Deposit Account Number:	50-1505/5119-13000/EBM
PROVISIONAL FILING FEE AMOUNT:	\$80.00

The invention was made by an agency of the United States Government or under a contract with an agency of the United States Government

- ☒ No.
- ☐ Yes, the name of the U.S. Government agency and the Government contract number are: _____

Respectfully submitted,

Signature 
Typed or Printed Name: Eric B. Meyertons

Date October 10, 2003
Registration No.: 34,876

☐ Additional inventors are being named on separately numbered sheets attached hereto

PROVISIONAL APPLICATION FILING ONLY

00746 U.S. PTO
60/510707



101003

PATENT

IN THE UNITED STATES PATENT AND TRADEMARK OFFICE

Application No.: Unknown
Filed: Herewith
Inventor(s):
Stephen Maldonado
Keith J. Stevenson

Title: CARBON NANOTUBE-
BASED
ELECTROCATALYTIC
ELECTRODES

§ Examiner: Unknown
§ Group/Art Unit: Unknown
§ Atty. Dkt. No: 5119-13000/EBM
§
§
§
§
§
§
§
§
§
§

CERTIFICATE OF EXPRESS MAIL
UNDER 37 C.F.R. §1.10

"Express Mail" mailing label number: EV324270544US
DATE OF DEPOSIT: October 10, 2003

I hereby certify that this paper or fee is being deposited with the
United States Postal Service "Express Mail Post Office to
Addressee" service under 37 C.F.R. §1.10 on the date indicated
above and is addressed to:

Commissioner for Patents
Alexandria, VA 22313-1450


Derrick Brown

FEE AUTHORIZATION

Commissioner for Patents
P.O. Box 1450
Alexandria, VA 22313-1450

The Commissioner is hereby authorized to charge the following fees to Meyertons, Hood, Kivlin,
Kowert & Goetzel, P.C. Deposit Account Number 50-1505/5119-13000/EBM

\$80.00 – Provisional Patent Application Filing Fee

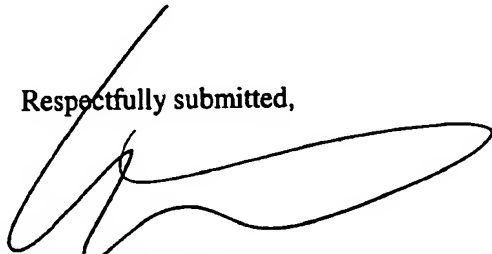
Total Amount: \$80.00

Attorney Docket No.: 5119-13000

Maldonado et al.

The Commissioner is also authorized to charge any extension fee or other fees which may be necessary to the same account number.

Respectfully submitted,

A handwritten signature in black ink, appearing to be 'Eric B. Meyertons', written over the text 'Respectfully submitted,'.

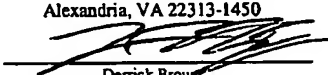
Eric B. Meyertons
Reg. No. 34,876

Attorney for Applicant

MEYERTONS, HOOD, KIVLIN, KOWERT & GOETZEL, P.C.
P.O. BOX 398
AUSTIN, TX 78767-0398
(512) 853-8800 (voice)
(512) 853-8801 (facsimile)

Date: 10-10-03

**PATENT
5119 - 13000**

CERTIFICATE OF EXPRESS MAIL UNDER 37 C.F.R. §1.10	
"Express Mail" mailing label number:	<u>EV324270544US</u>
DATE OF DEPOSIT:	October 10, 2003
I hereby certify that this paper or fee is being deposited with the United States Postal Service "Express Mail Post Office to Addressee" service under 37 C.F.R. §1.10 on the date indicated above and is addressed to:	
Mail Stop Provisional Patent Application Commissioner for Patents Alexandria, VA 22313-1450	
 Derrick Brown	

CARBON NANOTUBE-BASED ELECTROCATALYTIC ELECTRODES

By:

Stephen Maldonado

Keith J. Stevenson

Attorney Docket No.: 5119 - 13000

Eric B. Meyertons/JLM
Meyertons, Hood, Kivlin, Kowert & Goetzel, P.C.
P.O. Box 398
Austin, Texas 78767-0398
Ph: (512) 853-8800

BACKGROUND OF THE INVENTION

1. Field of Invention

A method for the direct preparation carbon nanofibers is disclosed. In an embodiment, the carbon nanofibers may be formed directly on a conductive substrate (e.g., nickel). Carbon nanofibers on a conductive substrate may be useful as electrodes. The carbon nanofibers may be formed by pyrolysis of iron (II) phthalocyanine. Carbon nanofiber prepared by methods disclosed herein exhibit certain electrochemical properties that may be desirable.

2. Description of Related Art

The literature for carbon-based electrodes is rich in studies with traditional forms of carbon (i.e., carbon blacks, pyrolytic graphite and glassy carbon). However, much less attention has been given to carbon nanofiber (CNFs) and carbon nanotube (CNTs) materials as electrocatalysts. CNFs and CNTs are largely classified together as a single type of carbon material. The term 'carbon nanotube' has been used as the main descriptor for various forms of tubular carbon of recent study. As used herein, a "CNT" refers to a carbon structure small enough to exhibit observable quantum effects (e.g., less than about 30 nm). As used herein, a "CNF" refers to a carbon structure too large to exhibit observable quantum effects (e.g., greater than about 30 nm). CNFs and CNTs may be collectively referred to as carbon nanostructures.

SUMMARY

In an embodiment, certain carbon materials may possess properties desirable for design of electrodes used for electrochemical devices. For example, carbon materials may exhibit relative high stability, conductivity, high surface area and chemical resistance. However, electrochemical oxidation and reduction of a variety of technologically-relevant analytes (e.g., oxygen, hydrogen, peroxide, methanol) may exhibit slow electron transfer kinetics with carbon electrodes. Numerous studies have focused on the mechanism of oxygen reduction for use in preparation of

electroanalytical sensors and electrochemical based technologies such fuel cells and batteries. Organometallics, e.g., metal phthalocyanines and metal porphyrins, have drawn considerable interest as catalytic modifiers for carbon-based electrodes (e.g., carbon blacks and glassy carbon) because they are known to lower the kinetic overpotential for oxygen reduction. Early studies in this area demonstrated that annealing of various metal macrocycles on carbon black increases their catalytic behavior but that at temperatures much beyond 650 °C their catalytic behavior is severely diminished. Interestingly, some metal tetraphenylporphyrin-loaded carbon black electrodes subjected to even higher heat stresses (>850 °C) to cause pyrolysis of the organometallic precursor have been reported catalytic performances close to that of commercial platinum particles. Pyrolyzed metal phthalocyanines on a carbon surface do not exhibit as great a catalytic behavior as low temperature annealed metal phthalocyanines, but their stability over repeated use is much better than low temperature annealed electrodes.

BRIEF DESCRIPTION OF THE DRAWINGS

Advantages of the present invention will become apparent to those skilled in the art with the benefit of the following detailed description of embodiment and upon reference to the accompanying drawings, in which:

Figure 1A depicts a low resolution, large area micrograph showing electrode structure of CNF electrodes prepared by pyrolysis of iron(II) phthalocyanine;

Figure 1B depicts a higher resolution micrograph of CNF electrodes prepared by pyrolysis of iron(II) phthalocyanine showing local micro-/nano-structure;

Figure 1C depicts a view normal to the substrate, showing vertical nanofiber alignment;

Figure 2A depicts a low magnification view of a nanotube showing numerous kinks along the length of a CNF prepared by pyrolysis of FePc showing bamboo-like structure;

Figure 2B depicts a high magnification micrograph of a nanotube illustrating the breaks in the graphene layers;

5 Figure 3 depicts x-ray photoelectron spectra for C1s and N1s core levels of CNF electrodes;

Figure 4 depicts a voltammetric response of a CNF electrode immersed in a deaerated aqueous solution of 0.1 M KNO_3 ;

10 Figure 5A depicts voltammetric response of a CNF electrode(solid line) and a bare nickel mesh electrode (dotted line) immersed in an aqueous solution containing 0.5 M KNO_3 after deaeration with Ar;

15 Figure 5B depicts voltammetric response of a CNF electrode immersed in an aqueous solution containing 0.5 M KNO_3 after O_2 saturation;

Figure 6A depicts a chronocoulometric response plot of Q vs $t^{1/2}$ (Anson plot) measured for solutions containing 1 M KNO_3 and indicated amounts of dissolved O_2 ;

20 Figure 6B and 6C depict a chronocoulometric response plot of Anson slope vs. dissolved O_2 concentration obtained over different concentration ranges;

Figure 7 depicts linear sweep voltammograms of a CNF electrode immersed in aqueous
25 solutions of pH: 5.5, 7.7, 9.0, 10.6, and 12.6;

Figure 8 depicts a plot of the apparent charge transfer coefficient, α'_{obs} , versus pH; and

Figure 9 depicts a voltammetric response of a CNF electrode immersed in an O₂ saturated aqueous solution containing 1M NaOH.

While the invention is susceptible to various modifications and alternative forms, specific
5 embodiments thereof are shown by way of example in the drawings and will herein be described
in detail. It should be understood that the drawing and detailed description thereto are not
intended to limit the invention to the particular form disclosed, but on the contrary, the intention
is to cover all modifications, equivalents and alternatives falling within the spirit and scope of the
present invention as defined by the appended claims.

DETAILED DESCRIPTION OF EMBODIMENTS

While several methods such as arc and laser deposition have been used for producing
carbon nanotubes (CNT) and carbon nanofibers (CNF), chemical vapor deposition (CVD)
15 methods may be more facile for large scale production of well defined carbon-based films and
arrays. In an embodiment, a method of forming carbon nanostructures may be based on the bulk
pyrolysis of metal phthalocyanines.¹⁴ Such synthesis methods may produce CNFs and CNTs that
are substantially aligned perpendicular the supporting substrate. Several investigators have
conducted electrochemical investigations of SWCNTs, MWCNTs and CNFs electrodes made by
20 spin coating suspensions onto conductive substrates. Others have relied upon gross transfer of a
carbon film from a growth substrate onto a conductive surface.¹⁵ In the former case, the films
formed by such spin coating methods typically include disordered mats of dense, randomly
entangled nanotubes. In the latter case, the effects of physical transfer and/or chemical
treatments on the carbon nanostructures may be poorly understood and/or recognized. To avoid
25 these complications, there has been a push to grow carbon nanostructure materials directly on
conductive substrates.

Embodiments presented herein include methods for direct preparation of substantially
vertically-aligned carbon nanofiber electrodes produced directly on a metallic substrate. Such

embodiments may be performed without excessive pre-treatment, post-treatment or chemical surface activation. A difference between carbon nanostructures formed by method disclosed herein and carbon nanostructures formed by physically transferring the nanostructures to a conductive substrate may be that carbon nanostructures that are directly grown on conductive substrates may not include a binding agent. An additional difference may be that where the nanostructures are to be used in electrodes, the carbon electrocatalyst properties of the nanostructures (i.e. orientation, alignment, crystalline, composition) may be tuned by adjustment of the pyrolysis protocol. Additionally, formation of electrodes by direct growth on a conductive substrate may provide an inherently easier, quicker, and/or more controllable method than the traditional methods for making high surface area carbon electrodes. Preliminary studies of carbon nanostructure electrodes prepared using iron (II) phthalocyanine demonstrate high electrocatalytic ability for the reduction of dissolved oxygen at neutral to basic pHs. The repeatability and stability of such carbon electrodes is excellent as signified by the electrodes' linear response to changes in dissolved oxygen

Experiments were conducted to form carbon nanostructures on a conductive substrate. Carbon nanostructures formed directly on a conductive substrate were then tested to assess the properties of the nanostructures as electrodes.

To grow the carbon nanostructures, nickel mesh (commercially available as Alfa Aesar, 100 mesh) was cut into 0.40 cm² squares prior to pyrolysis. The pyrolysis of iron(II) phthalocyanine (commercially available from Aldrich, and hereafter denoted as "FePc") on nickel mesh substrates was performed at 990° C in a reducing atmosphere of Ar-H₂ (99.997 and 99.95%, respectively, commercially available from Praxair). A gas flow reactor was used. The gas flow reactor included a quartz tube and a two zone reactor tube furnace. The quartz tube had an outer diameter about 35mm and an inner diameter about 32. The two zone tube furnace (commercially available from Thermcraft, model 2158-6-3ZH) was fitted with temperature controllers. Prior to growing the carbon nanostructures, the nickel mesh substrates were inserted into zone 2 of the furnace. The quartz tube was purged with Ar for ~10 minutes. Subsequently,

a mixture of Ar and H₂ gases (at about a 0.8:1 ratio) was introduced to the furnace. The gas flow was about 47 ccm (cubic centimeter per minute). During the gas purge, the two furnace zones were heated to designated temperatures. Specifically, zone 1 was heated to about 500 °C and zone 2 was heated to about 1000 °C. When the cooler (upstream) zone 1 reached 500 °C, 0.2 g of FePc was introduced and nanostructure growth was allowed to occur for about 5 minutes. The temperature of zone 1 was then raised up to about 1000° C and maintained at this temperature for about 15 minutes. The furnace was then turned off and the carbon nanofiber (CNF) electrodes were allowed to cool in the furnace until the temperature reached about 850 °C. The hydrogen gas flow was stopped while Ar flow was increased to 45 ccm to maintain an approximately constant total gas flow. The entire furnace was allowed to cool to room temperature under the Ar gas flow. The CNF electrodes were then removed from the quartz tube and stored in sealed gas tight vials pending structural and electrochemical characterization.

The carbon films of the CNF electrodes appeared on the nickel mesh substrate as a fine black felt-like or carpet-like layer. The nominal mass of carbon film prepared in this manner was about 1 mg. The carbon films adhered relatively strongly to the nickel. Scanning electron microscopy (SEM) of the resultant carbon nanotube films was carried out on a LEO 1530 operating at 10 kV. Transmission electron microscopy (TEM) was performed on a JEOL 2010F operating at 120 kV. TEM samples were prepared by first suspending collected nanotubes in ethanol and then placing a drop of the suspension on copper grid (200 mesh, PELCO) with a thin carbon coating. Surface analysis of the CNF was performed by X-ray photoelectron spectroscopy (XPS) using a PHI 5700 ESCA system equipped with Al K-alpha monochromatic (1486.6 eV) photons. Photoelectron spectra were recorded for the C1s, N1s, O1s, Fe2p_{1/2} and Fe2p_{3/2} core levels. All spectra are referenced to low, medium, and high photoelectron energy ranges using Au4f_{7/2}, Ag3d_{5/2} and Cu2p_{3/2} at 83.98, 368.27, and 932.67 eV, respectively.

A single glass compartment, three electrode, gas tight electrochemical cell was employed for cyclic voltammetry and chronocoulometry studies of the electrodes. Pt mesh (commercially available from Aldrich) and Hg/Hg₂SO₄ (saturated K₂SO₄, available from CH Instruments) were

used as counter and reference electrodes, respectively. Carbon nanofiber/nickel mesh or glassy carbon served as the working electrode. Glassy carbon electrodes (diameter = 5mm, Alfa Aesar) were fabricated by casting in resin (Epon 828, Resolution Performance Products) and polished with 1, 0.3, and 0.05 micron diameter alumina slurries prior to use. Geometric surface areas of the carbon nanofiber electrodes were determined by chronocoulometry (CC) using hexaammineruthenium (III) chloride (Strem Chemicals) in 1 M KNO₃. Bare nickel electrodes were stepped from -0.4V to -0.8V vs. Hg/Hg₂SO₄ (saturated K₂SO₄) for 1 second and the area was calculated from the slope ($m=2nFAD_0^{1/2}Cp^{-1/2}$) of the linear portion of the Q vs. $t^{1/2}$ plot (Anson plot) using the diffusion coefficient, $D_0=7.3 \times 10^{-7} \text{ cm}^2 \text{ s}$, determined by the steady state current ($i_{lim}=4nFD_0Cr$) of a platinum microelectrode with $r = 13 \text{ }\mu\text{m}$. For three bare nickel mesh electrodes, the observed electroactive area was $1.1 \pm 0.1 \text{ cm}^2$. Because the diffusion layer thickness for all measurements was sufficiently large ($(Dt)^{1/2} = 16 \text{ }\mu\text{m}$ for the shortest experimental time, $v=100 \text{ mV/s}$), the diffusion layer was assumed to follow the overall exposed nanofiber area rather than individual tubes. The geometric surface area of the CNF electrodes was taken to be the same area of the equivalent bare nickel mesh electrodes.

Solutions in absence or presence of O₂ were prepared by purging with either Ar or O₂ (99.5%, Praxair) introduced through a gas inlet of the electrochemical cell. Pressures and concentration of O₂ were measured using a mercury manometer connected to the cell. Dissolved oxygen concentrations were calculated using the Bunsen coefficient (i.e., Henry's Law constant) for oxygen solubility in 1 M KNO₃ at 25 °C.¹⁷ The diffusivity of dissolved oxygen, assumed to be $1.75 \times 10^{-5} \text{ cm}^2 \text{ s}^{-1}$,¹⁸ is used in calculations involving chronocoulometry (Anson slopes). The solution was stirred while the cell was being pressurized and prior to and after each electrochemical experiment.

For cyclic voltammetry and chronoamperometry studies, the aforementioned gases were bubbled through the test solutions for 20 minutes prior to the start of measurements (to fully purge and to fully oxygenate, respectively) and again for 1 minute in between measurements. Solution volumes were ~5-10 ml. The cell was kept at ambient pressure. Electrolyte solutions

were prepared using potassium nitrate (EM Science, 99.9%), sodium hydroxide (Aldrich, 99.99%), and/or boric acid (Spectrum, 99.9%) as received. The solutions with pH values 5.1 to 10.6 had formal concentrations of 0.9 M KNO₃ and 0.1 M HBO₃. The pH was adjusted by adding small aliquots of concentrated NaOH. The solution with a pH of 12.6 was made with 1 M KNO₃ and a small amount of NaOH added. The solution with a pH of 14 was 1 M NaOH.

Chronoamperometry studies were performed using a single potential-step method. The method stepped from an initial potential of -0.3 V to a final potential of -0.7 V potential. The charge passed for a period of one second was recorded. Cyclic voltammograms (CV) in the presence of oxygen were obtained by sweeping the potential from -0.2V to -0.9V at various sweep rates between 5 mV/s and 100 mV/s in corresponding supporting electrolytes presence of oxygen. All CVs conducted in the presence of oxygen were background subtracted. All electrode potentials are reported vs Hg/Hg₂SO₄ (saturated K₂SO₄) which is ca. 0.64 V positive of NHE. All electrochemical measurements were taken with a quiescent solution. The electrochemical cell temperature was held at a constant temperature (23 ± 0.5 °C) by placing in water bath. All electrochemical studies were performed with either a CH Instruments 700A potentiostat or an Autolab PGSTAT 30 interfaced to a PC.

In general, CNFs are produced via catalytic dehydrogenation of hydrocarbons (e.g., acetylene, xylene) over metallic catalyst nanoparticles (e.g., Fe, Ni, Co) dispersed on insulating substrates (e.g., SiO₂ and Alumina). In embodiments presented herein, organometallic precursors such as metallocenes and phthalocyanines (iron (II) phthalocyanine in this case) act as both the hydrocarbon source and decomposition catalyst to yield large quantities aligned nanofiber bundles.¹⁹ Using a modified synthesis scheme this approach may be adapted to prepare aligned CNF electrodes directly on conducting nickel mesh substrates. Scanning electron microscopy (SEM) studies (as shown in Figure 1) of CNFs prepared in this way, showed the homogenous distribution of nanofibers on the nickel surface with no discernable bare spots or uncoated regions observed. The produced material consists of carpet- or felt-like structures of carbon fibers that were fairly uniform and aligned normal to the nickel substrate. Fiber lengths were

generally greater than 10 μm and diameters ranging from about 40-60 nm. Higher magnification TEM images (shown in Figure 2) revealed the presence of hollow fibrils exhibiting irregular and interlinked corrugated features, consistent with other reports describing the preparation of nitrogen-doped nanotubes.²⁰ Straight segments of parallel aligned graphene sheets of the CNF appear crystalline and ordered over 10's of nm distances. These more crystalline domains intersect with more disordered regions and give rise to compartmentalized bamboo-like structures. These graphitic dislocations in the nanofiber correspond to sites where edge plane graphitic carbon is exposed at the sidewalls. TEM images also showed the occurrence of iron nanoparticles which appeared to be encapsulated with graphitic shells or within the CNF.

XPS analysis of the CNF electrodes (as depicted in Figure 3) indicates that the carbon is predominantly sp^2 hybridized as evidenced by the presence of a C1s binding energy of 284.7 eV, similar to that of HOPG.²¹ No detectable sidebands in the C1s region (285-291 eV) were evident to denote the presence of graphene oxides or oxygen containing functionalities on the CNF electrodes. A small O1s signal at 532.6 eV appeared to indicate the existence of physisorbed oxygen. Additionally, the presence of a N1s doublet at ~398.9 and 401.0 eV was consistent with the incorporation of nitrogen within the graphene sheets. In agreement with similar reports for CNTs grown by pyrolysis of other metal (cobalt and nickel) phthalocyanines,²² the binding energy centered at 398.9 eV corresponds to "pyridinic" nitrogen while that at 401.0 eV is commensurate with "pyrrolic" type nitrogen. The former refers to N atoms, which contribute to the π system with one p electron, while the latter refers to N atoms with two p electrons on the π system, although not necessarily coordinated in a five membered ring as pyrrole. A very weak peak at ~405 eV also exists that is consistent with presence of "graphitic" nitrogen, corresponding to highly coordinated N atoms substituting inner carbon atoms in the graphene sheets. A very weak doublet of peaks at 707 and 720 eV corresponding to the $\text{Fe}2\text{p}_{3/2}$ and $\text{Fe}2\text{p}_{1/2}$ signals was evident suggesting the presence of reduced iron species. No binding energy peaks within the range 700-740 eV were apparent to denote the existence of oxidized forms of iron (Fe^{2+} or Fe^{3+}). Integration of the relative N and Fe elemental abundances indicated that CNFs

contain roughly 1% (mass) nitrogen and 0.5% (mass) iron. Surface concentrations were mainly carbon with ~ 1% N atoms and ~0.1% Fe atoms.

Catalytic grown CNFs are known to be strongly hydrophobic as prepared. Typically, in order for these materials to be used in electrochemical applications involving aqueous electrolytes, the carbon electrode needs to be preconditioned or pretreated so that they are easily wettable when immersed in electrolyte. Harsh chemical or electrochemical oxidation methods that use concentrated nitric and sulfuric acids are typically employed to effectively introduce oxygen containing surface functionalities (carboxy and carboxylic anhydride groups). However, this abrasive treatment may lead to breakdown or fracture of the CNF nanostructure.²³ CNF electrodes prepared according to embodiments disclosed herein also do not easily wet. However, in an embodiment, mild electrochemical conditioning of such electrodes by cycling from -1.4 to +0.8 V vs Hg/HgSO₄ at 100 mV/sec in aqueous 1M KNO₃ for a period of about two minutes induces uniform wetting of the CNF electrodes. This is evidenced by a large increase in the voltammetric current during cycling when the entire carbon film fully saturates with electrolyte.

A typical voltammetric response for CNF electrodes immersed in deaerated solution containing 0.1 M KNO₃ is shown in Figure 4 for potential cycles between +0.8 and -0.8 V vs Hg/HgSO₄. Over most of the potential range, only capacitive charging currents are observed. A small anodic peak observed at +0.8 V is characteristic of nitrate insertion into the CNFs, broadly consistent with previous reports for voltammetric investigations of HOPG electrodes in similar electrolytes.²⁴ A broad cathodic wave is also seen in this potential range corresponding to the deintercalation of nitrate ions, indicating that the insertion process may be reversible. The CNF electrodes are very stable as no changes in the voltammetric response is observed for extended cycling between +0.8 and -0.8 V. Typically anion intercalation may be accompanied by formation of graphine oxide,²⁵ however, the appearance of no new voltammetric peaks to signify the formation of oxygen functionalities are observed after extended potential cycling. The mild conditioning step described in embodiments herein should not be confused with more rigorous electrochemical pretreatment activation (ECP) methods reported by McCreery and others. ECP

of HOPG electrodes in potassium nitrate solutions has been reported previously²⁶, but the conditions used in embodiments presented herein are much milder. For example, the CNF electrodes were cycled to much less extreme oxidation potentials, and much shorter time periods (cf. +0.8 V vs +2.2 V vs Hg/HgSO₄). The electrochemical activation step employed was enough
5 to overcome the strong hydrophobicity of the carbon films but was not enough to introduce oxygen surface functionalities or to damage the CNF structure. XPS and SEM analysis of wetted electrodes showed no changes in the overall CNF composition or structure. TEM analysis was inconclusive in determining if possible structural changes or defects were introduced after the wetting step. Regardless, from the available evidence, there appears to be no substantial amount
10 of oxygen functionalities inherent to or introduced to the CNF electrodes during electrochemical conditioning.

Figures 5A and 5B show representative CVs of CNF electrodes immersed in a 0.5 M KNO₃ solution for potential cycles between -0.4 and -0.8 V in the absence of oxygen (Figure 5A)
15 and presence of oxygen (Figure 5B). In the absence of oxygen, the voltammetric response exhibits only a capacitive response. It also can be seen that the current measured for a CNF coated nickel electrode is several orders of magnitude higher than that for the uncoated nickel electrode of the same area in oxygenated or deaerated solutions, indicating that the observed electrochemical response is inherent to the CNFs and not the underlying substrate. The CNF are
20 expected to exhibit larger background current signals than the bare nickel because the higher surface area leads to a higher overall capacitance. From Figure 5A, the capacitance of the films can be estimated to be roughly 11 F/g in potassium nitrate. The estimated capacitance is in agreement with the wide range of reported specific capacitance values ranging been 4 to 80 F/g²⁷ and 18 to 40 F/g²⁸ for electrolyte conditions similar to this study. Figure 5B shows that when the
25 carbon nanofiber films were cycled at a scan rate of 5mV/s in aqueous solutions saturated with O₂, a peak for the reduction of oxygen was observed near -0.5 V vs Hg/Hg₂SO₄.

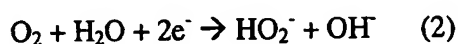
Potential step experiments were conducted to demonstrate that the carbon nanotube electrodes were sensitive to the oxygen content in solution. To best discern the faradaic response

from the large capacitive charging of the electrodes, chronocoulometry was used. With chronoamperometry or cyclic voltammetry, the measured signal is a combination of the faradaic and capacitive currents. Distinguishing the two components may be difficult for electrodes with a large capacitance. Chronocoulometry allows the effects from the two processes to be readily discerned. It has been shown that after an initial time for the electrode surface to charge, a plot of the total charge passed vs. $t^{1/2}$ (Anson plot) is linear and a result of the faradaic process.²⁹

$$Q = 2nFAD_o^{1/2}\pi^{-1/2}t^{1/2} \quad (1)$$

The slope of the linear portion is then directly proportional to the concentration of dissolved oxygen and is independent of the material capacitance, as shown Figure 6A. As previously described, the concentration of dissolved oxygen can be estimated from the partial pressure of oxygen above the solution by way of Henry's Law. Controlling the oxygen partial pressure in the cell allowed for chronocoulometric measurements in the ppm oxygen concentration ranges. Figures 6B and 6C show that the change in Anson plot slopes over the studied concentration ranges was linear. The number of electrons for the observed responses was 2.3, consistent with a $2e^-$ reduction to peroxide species.

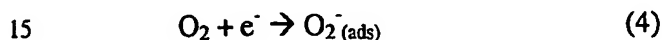
For neutral to alkaline pH values, oxygen is irreversibly reduced to hydrogen peroxide on unmodified carbon surfaces.



$E^0 = -0.065V$ (vs. NHE) For a given scan rate, $E_{p/2}$, (potential where the current is half the peak current) is more or less fixed but at more alkaline environments $E_{p/2}$ shifts more negative. For an irreversible $1e^-$ reduction or an overall ne^- reduction pathway with a $1e^-$ irreversible reduction as the rate determining step, the difference between the peak potential, E_p , and $E_{p/2}$ is given by:³⁰

$$E_{p/2} - E_p \equiv \frac{1.857RT}{\alpha_{obs}F} \quad (3)$$

While the direct application of this equation to the reduction of oxygen on most carbon surfaces is inappropriate, it does serve as a reminder that the peak width of the obtained
 5 voltammograms should change if the observable transfer coefficient α_{obs} changes (e.g., the kinetics of the reduction change.) Figure 7 also shows that the peak width of the reduction wave is broad and roughly constant in slightly acidic to neutral pH solutions but sharpens significantly in increasingly more alkaline environments. The peak widths for a set of scans for a given pH solution may be used to roughly gauge α_{obs} by using Equation 1, as seen in Figure 8. A similar
 10 trend was noted with glassy carbon surfaces that had undergone various pretreatments.³¹ α_{obs} may increase with increased alkalinity on glassy carbon surfaces with a large number of adsorption sites.³² The availability of a large number of adsorption sites may allow the reduction of dioxygen to superoxide to become the rate determining step in strongly alkaline environments.



Although the exact nature of adsorption sites is not understood, it is clear that high defect carbon surfaces show a greater activity for oxygen reduction. It has been noted that in aqueous solutions the observed current densities for oxygen reduction on the basal plane of stress
 20 annealed pyrolytic graphite is lower than on glassy carbon or ordinary pyrolytic graphite.³³ It has been demonstrated that HOPG surfaces with greater specific capacitances required a lower overpotential for the oxygen reduction wave,³⁴ with the understanding that the larger the number of defects (e.g., exposed edge plane graphitic planes) on an HOPG surface, the larger the specific capacitance. If adsorption sites are related to edge plane graphite planes, then a surface with a
 25 large amount of exposed edge plane graphite should exhibit considerable oxygen reduction activity. Such kinks are evident in the TEM images of nanotubes described herein. Each dislocation is a site of exposed edge plane graphite. Adsorption of oxygen on the carbon nanofibers disclosed herein was evident in the first voltammogram obtained after bubbling

oxygen gas through the test solution for 20 minutes. Figure 9 shows that the first voltammogram was noticeably larger than the following scans at the same scan rate. The presumed reason for the larger initial observed current is adsorption of oxygen onto the carbon surface. Subtraction of a second scan voltammogram from the first scan voltammogram showed a symmetric gaussian peak, the 'extra' adsorbed oxygen. No attempt was made to quantify the amount of adsorbed oxygen as it seemed to be dependent on solution conditions and allotted time of oxygenation. The timescale for the oxygen adsorption was thought to be slow, as the one minute interval between successive scans was not enough to show a larger current. Therefore, it is consistent that carbon nanotubes with a large density of kinks per unit length should show considerable activity for oxygen reduction. This insight is not enough to explain all of the observed voltammetric features but is an obvious structural characteristic of carbon nanotubes which of yet has been poorly described in the carbon nanotube literature of electrochemical studies. There is one report in the literature noting possible electrocatalytic properties of some unspecified type of MWCNTs for the reduction of oxygen,³⁵ but the condition of the electrode (mixture of carbon nanotubes with liquid paraffin) and the ill-defined voltammetry makes it difficult to ascertain the electrocatalytic effect, if any, of that carbon nanotube material. Another observed feature of the voltammograms in this report is that the peak potential shifted slightly at neutral pH but shifted more negative with increased alkalinity. This is in contrast to the behavior of conventionally polished glassy carbon electrodes. Conventionally polished glassy carbon electrodes have been shown to exhibit a complex dependence on solution pH involving the transition of two distinct reduction waves³⁶, attributed to the reduction of oxygen with and without adsorption of superoxide species. The generalized behavior of glassy carbon is that the voltammograms become sharper in peak width and occur at a more positive potential in alkaline solutions. It is interesting to note that in very alkaline solutions (pH > 10), the reduction wave of the carbon nanotubes disclosed herein occurred at nearly the same potential of conventionally polished glassy carbon.

Comparisons of the CNF electrodes to earlier reports of transition metal macrocycle modified carbon electrodes, which have been studied extensively for catalytic behavior in fuel

cell applications, may be appropriate because both systems represent large surface area carbon electrodes. FePc was adsorbed onto Vulcan XC-72 carbon in a study that showed that the adsorbed organometallic complex shifted the reduction wave well positive ($\sim 0.5V$) of the reported values for most unmodified carbon surfaces.³⁷ The catalytic behavior was attributed to the ability of the iron centers to coordinate with dissolved dioxygen. It was a concern in the present study that residual FePc was present, despite the fact that the growth temperature used was well above the temperature where the molecule is known to completely breakdown, particularly the iron-nitrogen bonds.⁶ Capacitive voltammograms in Ar purged solution in 1 M NaOH showed neither of the described³⁸ reversible waves for the $Fe^{3+/2+}$ couple or the $Fe^{2+/0}$ couple of bulk iron (II) phthalocyanine on XC-72 carbon. Therefore, it is believed that the observed electrochemical response is not due to residual FePc.

At least two other factors should be considered when comparing CNF electrodes to other carbon materials. There is considerable nitrogen content in these carbon nanotubes and there are still iron nanoparticles present within the tube walls. Nitrogen incorporation in graphene sheets is thought to dramatically affect the catalytic ability of graphitic carbon in electron transfer reactions.³⁹ The electron transfer kinetics of the CNF electrodes were also examined using of two well known redox couples. Five different electrodes were studied and, scan rates for each electrode were recorded at 25, 50, 75, and 100 mV/s. For pooled electrodes, peak splittings for $Ru(NH_3)_6^{3+/2+}$, were 57 ± 6 mV while for $Fe(CN)_6^{3-/4-}$ were 55 ± 2 mV, indicative of nearly ideal nernstian conditions and rapid charge transfer kinetics. In contrast, for MWCNT electrodes prepared by Meyappan et al., measured peak splittings ranging from 100-168 mV for $Fe(CN)_6^{3-/4-}$ in 1 M KCl were observed to be a strong function of scan rate. Marken et al. reported similar peak splittings values of 168 mV for $Ru(NH_3)_6^{3+/2+}$ for MWCNT electrodes. Using microelectrode fashioned from a small bundle MWCNTs, Ayajan measured ~ 59 mV peak splittings for $Fe(CN)_6^{3-/4-}$ in unspecified electrolyte. In general, only ideal behavior is observed for carbon based electrodes after significant electrode pretreatment or activation. Fast electron transfer kinetics of embodiments disclosed herein (inferred from the nearly ideal nernstian response) suggest that the electron-conducting properties of CNF may be enhanced when doped

with N as a result of additional lone pairs of electrons that act as donors with respect to the delocalized π system of the hexagonal graphene network. This may well attribute to the low oxygen reduction overpotential necessary in neutral pH solutions and the increased necessary overpotential in alkaline environments. The nitrogen should play a role in determining the surface functionalities, particularly at higher pHs. Although the voltammetry does not indicate a significant amount of redox active surface groups, any surface groups present may play a strong role in electrocatalytic behaviors. In experiments discussed herein, the iron/nitrogen content in the nanofiber electrodes was not optimized; rather, it was kept constant for the samples considered. TEM analysis showed that the iron nanoparticles still present in the nanofibers were predominantly encased in graphite sheets. The background voltammograms exhibited no faradaic signals that could be attributed to iron oxidation.

References

1. M. A. T. Gilmartin, J. P. Hart, *Analyst*, 1995, 120, 1029.
2. For example, P. Brito, C. Sequeria, *J. Power Sources*, 1994, 52, 1.
3. A. Van Der Putten, A. Elzing, W. Visscher, and E. Barendrecht, *J. Electroanal. Chem.*, 1987, 221, 95.
4. K. Wiesner, *Electrochim. Acta*, 1986, 31(8), 1073.
5. G. Lalande, G. Faubert, R. Côté, D. Guay, J.P. Dodelet, L.T. Weng, P. Bertrand, *J. Power Sources*, 1996, 61, 227.
6. Ito, T.; Sun, L.; Crooks, R. M.; *Electrochem. Solid-State Lett.*, 2003, 6(1), C4.
7. Biro, L. P.; Bernardo, C. A.; Tibbetts, G. G.; Lambin, P.; *Proceedings of the NATO Advanced Study Institute on Carbon Filaments and Nanotubes: Common Origins, Differing Applications*, Kluwer Academic Publishers, Netherlands, 2001 p. 51-61.
8. De Jong, K. P.; Geus, J. W.; *Catal. Rev. Sci. Eng.*, 2000, 42(4), 481.
9. For instance, (a) Cadek, M.; Murphy, R.; McCarthy, B.; Drury, A.; Lahr, B.; Barklie, R. C.; in *het Panhuis, M.; Coleman, J. N.; Blau, W. J. Carbon* 2002, 40(6), 923. (b) Ebbesen, T. W.; Ajayan, P. M. *Nature* 1992, 358(6383), 220. (c) Journet, C.; Maser, W. K.; Bernier, P.; Loiseau, A.; Lamy de la Chapells, M.; Lefrant, S.; Deniard, P.; Lee, R.; Fischer, J. E. *Nature* 1997, 388(6644), 756.
10. Guo, T.; Nikolaev, P.; Thess, A.; Colbert, D. T.; Smalley, R. E. *Chemical Physics Letters* (1995), 243(1,2), 49.

11. Sinnott, S. B.; Andrews, R. *Crit. Rev. Solid St. Mat. Sci.* 2001, 26, 145.
12. De Jong, K. P.; Geus, J. W. *Catal. Rev. Sci. Eng.* 2000, 42, 481.
13. Rodriguez, N. N. *J. Mater. Res.* 1993, 8, 3233.
14. Huang, S.; Dai, L.; Mau, A. W. H.; *J. Phys. Chem. B.*, 1999, 103, 4223.
- 5 15. For example, (a) Niu, C.; Sichel, E. K.; Hoch, R.; Moy, D.; Tennent, H.; *Appl. Phys. Lett.*, 1997, 70(11), 1480. (b) J. Barisci, Wallace, G.G.; Baughman, R. H.; *J. Electrochem. Soc.* 2000, 147, 4580. (c) Hughes, M.; *Adv. Mat.*, 2002, 14, 382.
- 10 16. For example, (a) Murphy, M. A.; Wilcox, G. D.; Dahm, R. H.; Marken, F.; *Electro. Com.*, 2003, 5, 51. (b) Zhao, J.; Gao, Q.Y.; Gu, C.; Yang, Y.; *Chem. Phys. Lett.*, 2002, 358, 2002. (c) Luo, Y.; Vander Wal, R.; Hall, L. J.; Scherson, D.A.; *Electrochem. Solid St.*, 2003, 6(3), A56 (d) Chem, J. H.; Li, W. Z.; Wang, D. Z.; Yang, S. X.; Wen, J. G.; Ren, Z. F.; *Carbon*, 2002, 40, 1193. (e) Li, J.; Cassell, A.; Delzeit, L.; Han, J.; Meyyappan, M.; *J. Phys. Chem. B*, 2002, 106, 9299. (f) Smiljanic, O.; Dellerio, T.; Serventi, A.; Lebrun, G.; Stansfield, B. L.; Dodelet, J. P.; Trudeau, M.; Desilets, S.; *Chem. Phys. Lett.*, 2001, 342, 503.
- 15 17. MacArthur, C. G.; *J. Phys. Chem.*, 1916, 20, 495.
18. Xu, J.; Huang, W.; McCreery, R. L.; *J. Electroanal. Chem.*, 1996, 410, 235.
19. For a recent review see, Rao, C. N. R.; Govindaraj, A. *Acc. Chem. Res.* 2002, 35, 998.
- 20 20. (a) Wang, X.; Hu, W.; Liu, Y.; Long, C.; Xu, Y.; Zhou, S.; Zhu, D.; Dai, L. *Carbon*, 2001, 39, 1533. (b) Czerw, R.; Terrones, M.; Charlier, J.-C.; Blasé, X.; Foley, B.; Kamalakaran, R.; Grobert, N.; Terrones, H.; Tekleab, D.; Ajayan, P. M.; Blau, W.; Ruhle, M.; Carroll, D. L. *Nano Lett.* 2001, 1, 457.
21. Poirier, D. M.; Weaver, J. H.; *Surf. Sci. Spectra*, 1994, 2(3), 232.
- 25 22. Yudasaka, M.; Kikuchi, R.; Ohki, Y.; Yoshimura, S.; *Carbon*, 1997, 35(2), 195.
- 23 Ros, T. G.; Van Dillen, A. J.; Geus, J. W.; Koningsberger, D. C. *Chem. Eur. J.* 2002, 8, 1151.
24. Goss, C. A.; Brumfield, J. C.; Goss, C. A.; Irene, E. A.; Murray, R. W.; *Anal. Chem.*, 1993, 65, 1378.
- 30 25. Alsmayer, D. C., McCreery, R. L., *Anal. Chem.*, 1992, 64, 1528.
26. Engstrom, R. C.; Strasser, V. A.; *Anal. Chem.*, 1984, 56, 136.
27. Frackowiak, E.; Metenier, K.; Bertagna, V.; Beguin, F; *Appl. Phys. Lett.*, 2000, 77(15), 2421.
28. Barisci, J.; Wallace, G.; Baughman, R.; *J. Electrochem. Soc.*, 2000, 147(12), 4580.

29. Anson, F.; Anal. Chem., 1966, 38, 54.
30. Bard, A. J.; Faulkner, L. R.; Electrochemical Methods, 2nd Ed. John Wiley & Sons, New York, 2001 p.
31. Taylor, R. J.; Humffray, A. A.; J. Electroanal. Chem., 1975, 64, 95.
- 5 32. Yang, H.H.; McCreery, R.L.; J. Electroanal. Chem., 2000, 147(9), 3420.
33. Morcos, I.; Yeager, E.; Electrochim. Acta., 1970, 953.
34. Xu, J.; Huang, W.; McCreery, R. L.; J. Electroanal. Chem., 1996, 410, 235.
35. Britto, P. J.; Santhanam, K. S. V.; Rubio, A.; Alonso, J. A.; and Ajayan, P. M.; Adv. Mat., 1999, 11(2), 154.
- 10 36. Taylor, R. J.; Humffray, A. A.; J. Electroanal. Chem., 1975, 64, 95.
37. Tanaka, A. A.; Scherson, F. D.; Yeager, E. B.; J. Phys. Chem., 1987, 91, 3799.
38. Scherson, D. A.; Fierro, C. A.; Tryk, D.; Gupta, S. L.; Yeager, E. B., Eldridge, J.; Hoffman, R. W.; J. Electroanal. Chem., 1985, 184, 419.
39. Strelko, V. V.; Kuts, V. S.; Thrower, P. A.; Carbon, 2000, 38, 1499.

15 Further modifications and alternative embodiments of various aspects of the invention may be apparent to those skilled in the art in view of this description. Accordingly, this description is to be construed as illustrative only and is for the purpose of teaching those skilled in the art the general manner of carrying out the invention. It is to be understood that the forms

20 of the invention shown and described herein are to be taken as the presently preferred embodiments. Elements and materials may be substituted for those illustrated and described herein, parts and processes may be reversed, and certain features of the invention may be utilized independently, all as would be apparent to one skilled in the art after having the benefit of this description to the invention. Changes may be made in the elements described herein without

25 departing from the spirit and scope o the invention as described in the following claims. In addition, it is to be understood that features described herein independently may, in certain embodiments, be combined.

WHAT IS CLAIMED IS:

1. A method of forming a catalytic carbon nanofiber electrode, the method comprising:
preparing a conductive substrate; and pyrolyzing an organometallic compound in the
5 presence of the conductive substrate such that carbon nanotubes are grown directly on the
surface of the conductive substrate by a vapor deposition process.
2. The method of claim 1, wherein other organometallic compounds allow for carbon
nanofibers doped with non-carbon atoms.
- 10 3. The method of claim 1, wherein the use of iron (II) phthalocyanine which contains
carbon, nitrogen, and iron allows carbon nanofibers consisting of carbon, nitrogen, and
iron.
- 15 4. The method of claim 1, wherein the organometallic compound in the presence of the
conductive substrate further comprises reacting the organometallic compound in an
atmosphere comprising argon and hydrogen gases.
- 20 5. The method of claim 1, wherein the conductive substrate comprises nickel or platinum
mesh.
6. The method of claim 1, where in a method of separating a carbon nanofiber film from the
conductive growth substrate to produce 3D conduits of carbon nanofiber ensembles via
soaking in concentrated HNO_3 or aqua regia.
- 25 7. The process as a result of claim 1, wherein the oxygen reduction catalyst is atomically
dispersed and comprises material consisting of carbon, nitrogen, and iron, and/or other
materials but not limited to nickel, platinum, molybdenum, titanium, ruthenium,
manganese, sulfur and alloys, oxides or mixtures thereof.

8. A process for producing an electrode for an electrochemical device including a three dimensional catalytic ensemble of carbon nanofibers comprising the direct growth and dispersion of carbonaceous materials and catalyst by vapor deposition of organometallics.

5

9. The method of claim 1 wherein, the doped carbon nanofiber film is catalytically active to solution or gas phase species but not limited to the decomposition of hydrogen peroxide to oxygen in aqueous solutions.

10 10. A result of claim 7, the overpotential necessary for the reduction of oxygen in aqueous solutions is thermodynamically lowered than on traditional forms of carbon such as conventionally polished glassy carbon.

15 11. A result of claim 7, the repeatability of oxygen reduction on the carbon nanofiber electrodes is improved and lifetime extended by the catalytic elimination of hydrogen peroxide to oxygen.

20

ABSTRACT

CNF electrodes disclosed herein may be conveniently prepared on conductive substrates
5 by pyrolysis of iron (II) phthalocyanine in a reducing atmosphere. Such electrodes may possess
suitable properties for preparation of electrocatalytic electrodes and electrochemical sensors.
High surface area nitrogen doped CNFs prepared according to certain embodiments are
conductive and may exhibit high stability and improved catalytic activity for O₂ reduction in
aqueous solutions.

10

15

Fig. 1A

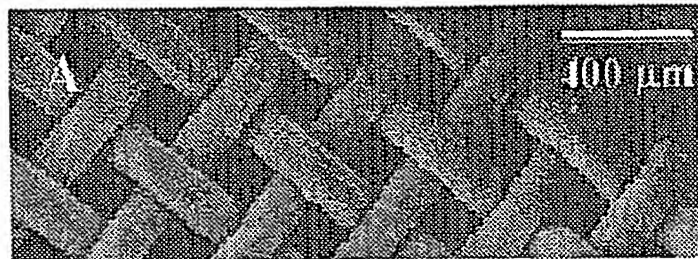


Fig. 1B



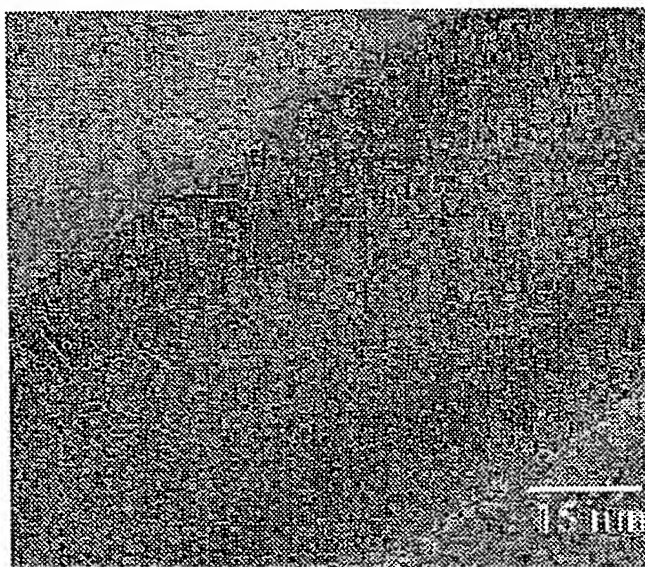
Fig. 1C



Fig. 2A



Fig. 2B



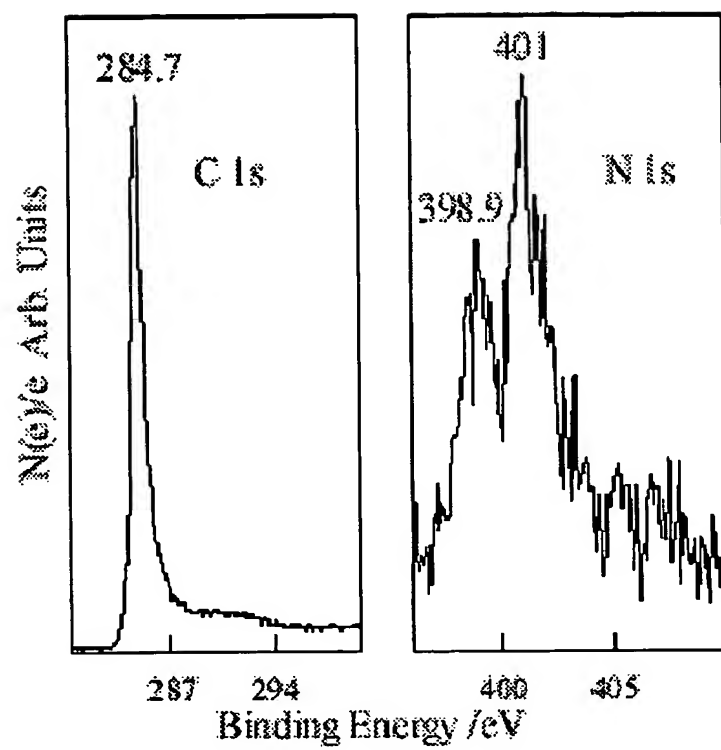


Fig. 3

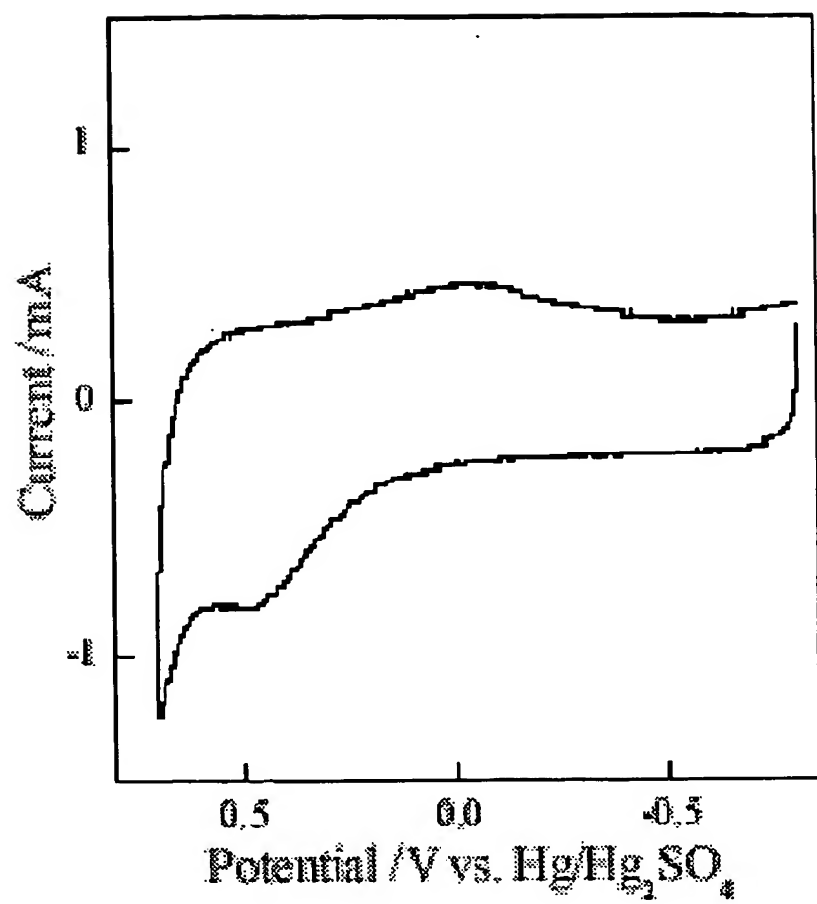


Fig. 4

Fig. 5A

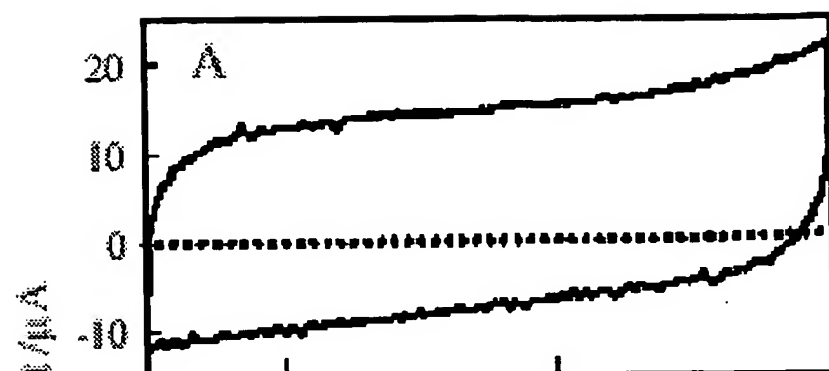


Fig. 5B

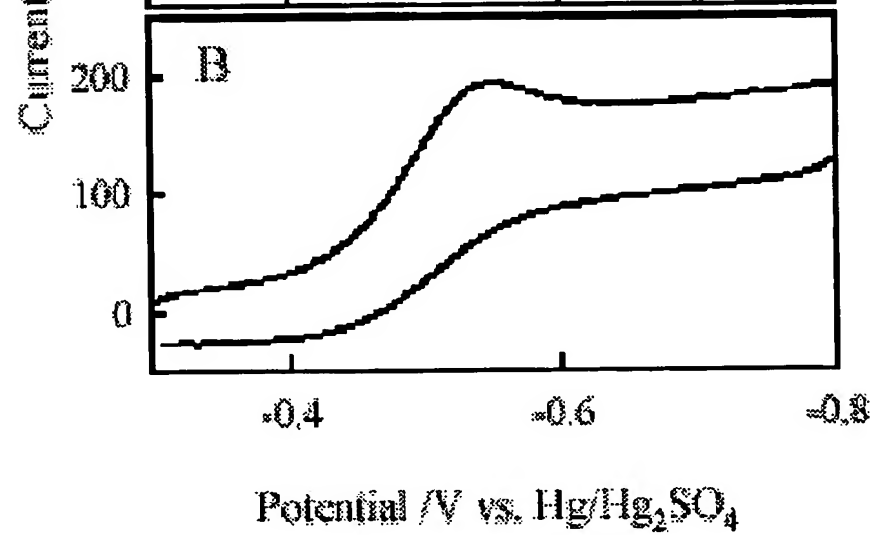


Fig. 6A

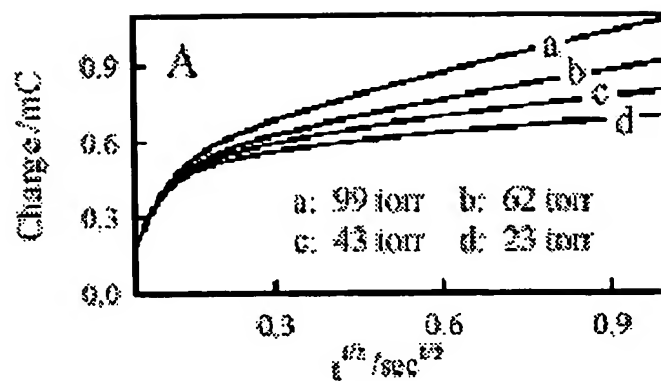


Fig. 6B

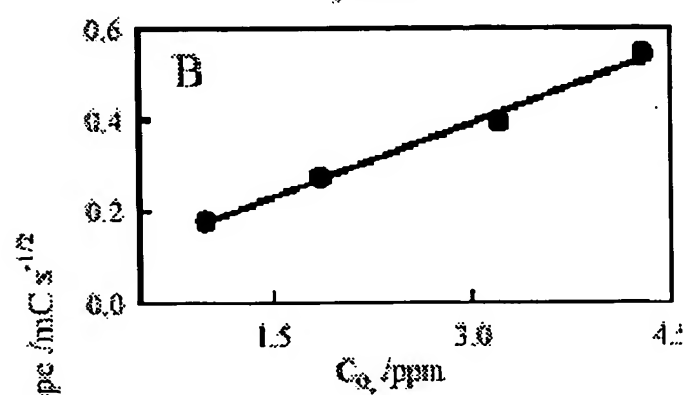
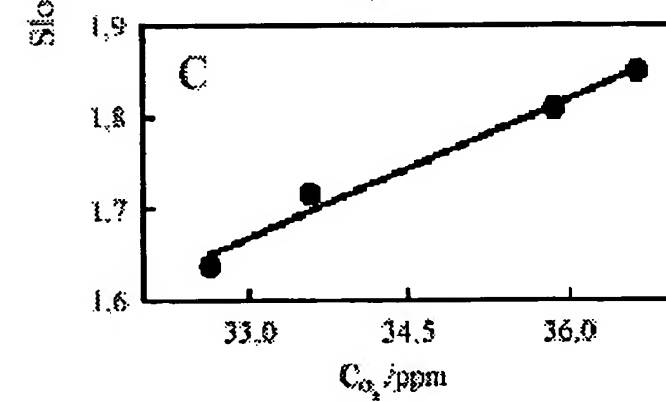


Fig. 6C



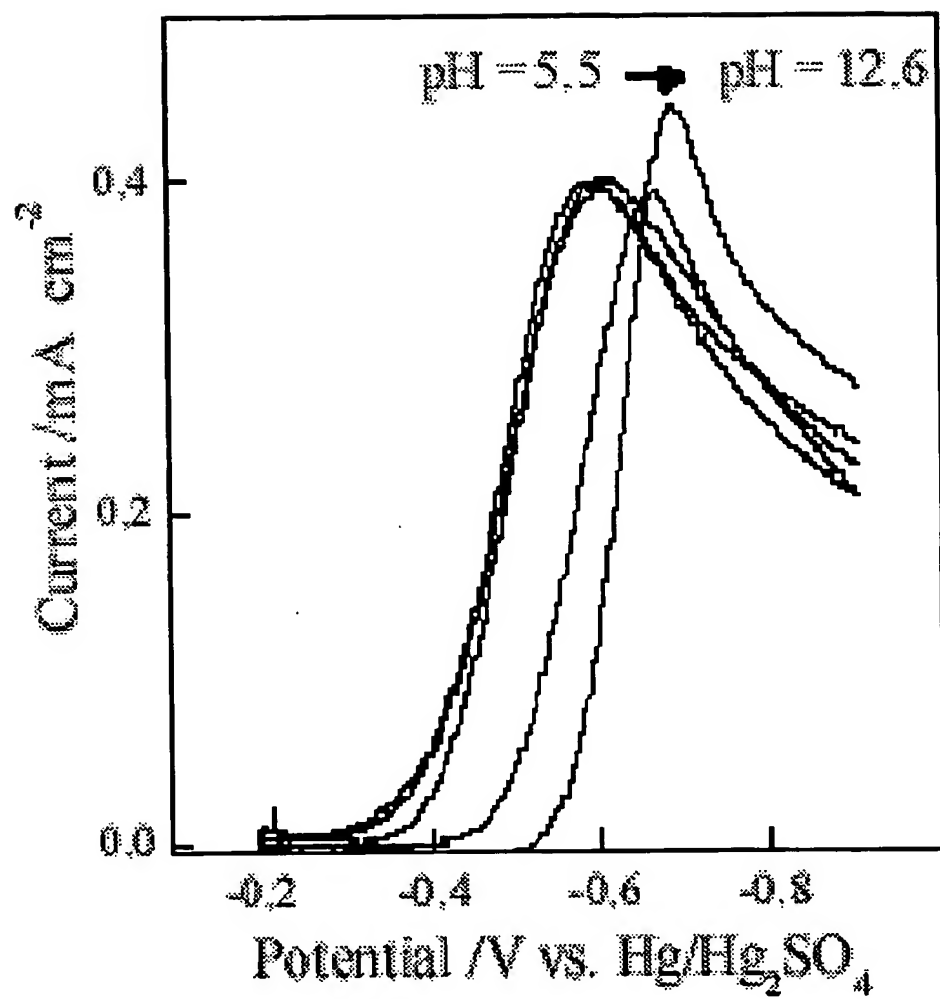
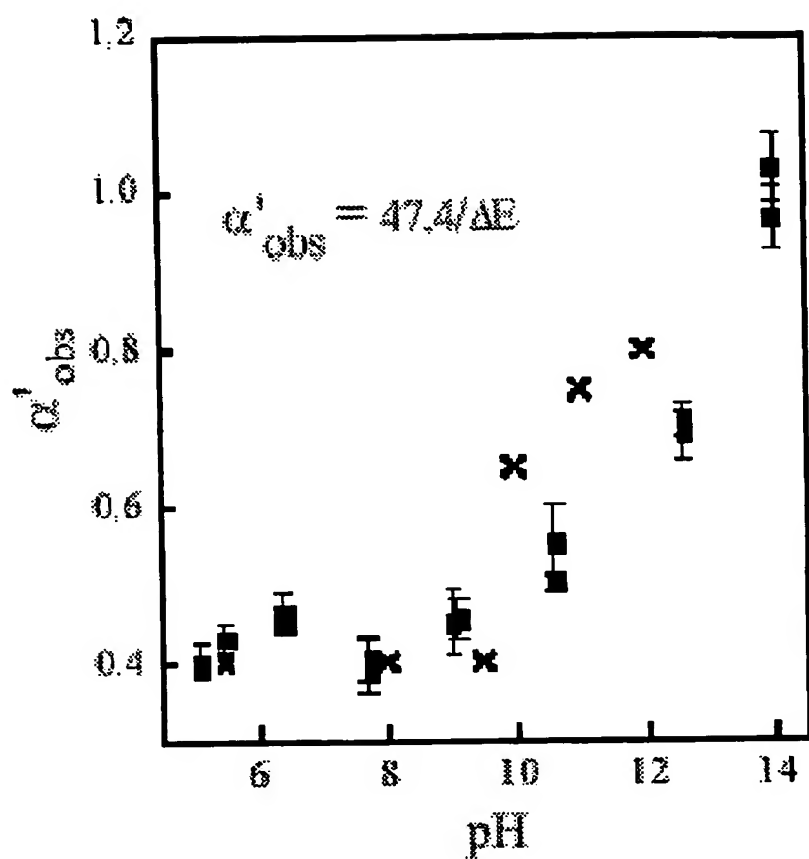
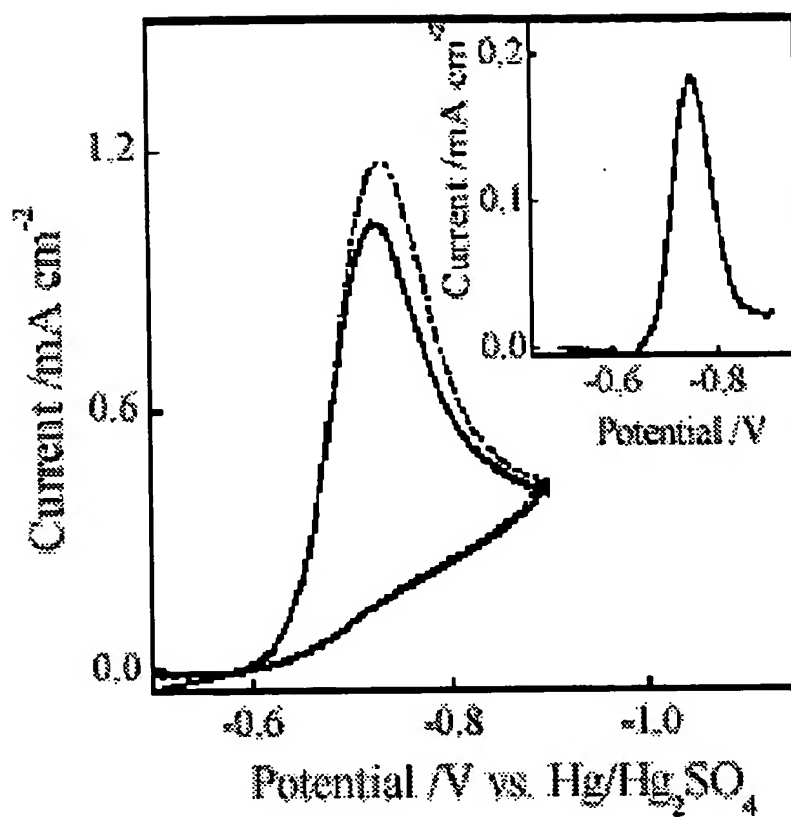


Fig. 7



Square symbols with error bars represent experimental data. Crossed symbols represent data from the literature for a similar experiment using borate buffer.

Fig. 8



The dashed voltammogram was initially recorded following 20 minute oxygenation step. The solid voltammogram was obtained after an additional 1 minute of oxygenation. Inset: Subtraction of the first (dashed) voltammogram from the second (solid).

Fig. 9

Document made available under the Patent Cooperation Treaty (PCT)

International application number: PCT/US04/033602

International filing date: 12 October 2004 (12.10.2004)

Document type: Certified copy of priority document

Document details: Country/Office: US
Number: 60/510,707
Filing date: 10 October 2003 (10.10.2003)

Date of receipt at the International Bureau: 13 January 2005 (13.01.2005)

Remark: Priority document submitted or transmitted to the International Bureau in compliance with Rule 17.1(a) or (b)



World Intellectual Property Organization (WIPO) - Geneva, Switzerland
Organisation Mondiale de la Propriété Intellectuelle (OMPI) - Genève, Suisse